Hittite Journal of Science and Engineering, 2018, 5 (Special Issue: Selected Papers from ULIBTK'17) 09-14
ISSN NUMBER: 2148-4171
DOI: 10.17350/HJSE19030000114

Dynamic Performance Comparison Of R134a and R1234yf Refrigerants for a Vapor Compression Refrigeration Cycle

Mert Sinan Turgut **Mustafa Turhan Çoban**
Ege University, Department of Mechanical Engineering, İzmir, TURKEY

Article History:
Received: 2018/01/19
Accepted: 2018/02/27
Online: 2018/09/07

***Correspondence to**: Mert Sinan Turgut, Ege University, Department of Mechanical Engineering*
E-mail: sinanturgut@me.com

ABSTRACT

Machines like air conditioners and refrigerators, which cause significant energy consumption in countries around the world, are widely used in industry and residences. Analyzing and studying the behavior of these machines with computer simulations can optimize performance of them. In this study, thermodynamic modelling and dynamic simulation of a vapor compression refrigeration cycle is handled. R134a and R1234yf are used as the primary fluid and water is used as the secondary fluid in the refrigeration cycle. R1234yf is a refrigerant, which has low Global Warming Potential (GWP) and Ozone Depletion Potential (ODP) and is recently has been begun to use as a substitute of R134a. In this study, dynamic behaviors of these two refrigerants are examined in a vapor compression refrigerant cycle with fixed operating conditions. Finite Difference Method is utilized for the modelling of the evaporator and condenser and Gungrr-Winterton and Travis et al. correlations are used for the modelling of the evaporation and condensation proccesses respectively. Orifice equation is utilized for the modelling of the expansion valve and modelling of the compressor is carried out by first dynamically simuating the heat transfer between the gas and surroundings until the gas reaches to compression chamber and after that the polytropic compression process in the chamber. For the realization of the dynamical simulation, refrigerant fluid mass flow rate is applied to the system as step input. Response of the system to the input is observed with transient p-h and coefficient of performance (COP) diagrams. The results showed that COP is started off with the values of 2.079 for R134a and 1.711 R1234yf, reached the maximum points of 2.577 for R134a and 2.02 for R1234yf, then slowly declined with fluctuations. In the p-h diagram, due to temperature rise of inner walls of the evaporator and condenser, condenser outlet and compressor inlet enthalpy values started off with 395,945 kJ/kg and 231,714 kJ/kg for R134a, 361,557 kJ/kg and 230,750 kJ/kg for R1234yf, then approached to the saturation curve with time and reached the values of 393,957 kJ/kg and 233,808 kJ/kg for R134a, 359,547 kJ/kg and 231,917 kJ/kg for R1234 yf.

Keywords:
Refrigeration cycles; Dynamic Simulation; System Modelling; Thermodynamics; Global Warming Potential

INTRODUCTION

Nowadays, refrigeration machines have various domestic and industrial applications and they play a huge role in energy consumption. By doing research studies, it is desired to make these machines more effective with less energy consumption [1]. Inspecting the dynamical behavior of the refrigeration machines is an important factor in design and control of these machines.

An important factor that affects the performance of the refrigeration machines is refrigerant selection [2]. Nowadays, refrigerants that have lower Global Warming Potential (GWP) and Ozone Depletion Potential (ODP) values are begun to take the place of those that have higher GWP and ODP values. In refrigeration machines, usage of R1234yf as an alternative to R134a, which is a refrigerant that is widely used in refrigeration machines, is gaining momentum due to its lower GWP and ODP values.

M.S. Turgut, M.T. Coban / Hittite J Sci Eng, 2018, 5 (Special Issue: Selected Papers from the 21st National Thermal Sciences and Technology Congress) 09–14

One of the first studies in dynamical modelling of the refrigeration cycles is conducted by the American National Standarts Bureau which investigated the steady-state behavior of the chiller [3] and boiler [4]. Moreover, the first studies that aim to optimize the system design and increase the energy saving have taken their place in the literature [5-7]. Chi and Didion [8] developed a software that can achieve the dynamical analysis of their heat pump called TRPUMP and includes the models of the all components in lumped parametric form and they compared the results that they acquired from the software with the results reported by the American National Standarts Bureau. Bonne et al. [9] studied the dynamical simulation of a heat pump with a compressor driven by an electrical motor and its on-off control. MacArthur [1] modelled a vapor compression cycle to accomplish the closed-loop control of the system, achieved the dynamic simulation, investigated the stability and response of the system and then compared these results with the experimental results. Chen and Lin [10] studied the optimal component combination to decrease the energy consumption of a small-scaled refrigeration system. In this study, the authors aimed to find the most favorable design combination of the compressor, the evaporator, the condenser and the capillary tube in order to reduce the energy consumption. Fu et al. [11] achieved the dynamical modelling of a dual-mode air-to-water heat transfer based heat pump. The studies in this field are published over time and still continuing with developing control strategies [12] and dynamical modelling of various system variations [13].

The effect of R1234yf and R1234ze refrigerants, which are recommended as a substite of the R134a, to the performance of the system are still studied. Yataganbaba et al. [2] studied the exergetic analysis of two-compressor refrigeration cycle with R1234yf and R1234ze refrigerants and compared the exergetic behavior of these two refrigerants. Mota-Babiloni [14] studied the effects of R134a, R1234yf and R1234ze refrigerants both experimentally and theoretically to the system performance, condenser outlet temperature and evaporator outlet temperature. Belman-Flores et al. [15] experimentally studied the effects of R1234 yf and R134a to the performance and evaporator and condenser outlet temperatures of a domestic refrigerator.

In this study, a vapor compression refrigeration cycle is considered. Thermodynamic and dynamical modelling of the system is achieved. R134a and R1234yf refrigerants are considered as the primary fluids and water is considered as the secondary fluid. Evaporator and condenser is modelled with the finite difference method and evaporation and condensation processes is modelled with Gungor and Winterton [16] and Travis et al. [17] correlations respectively. Modelling of the compressor is accomplished with two separate processes. First, until the refrigerant arrives to the compression room, the heat transfer between the refrigerant and the environment is considered. Then the polytropic compression process equation is utilized after the refrigerant arrives to the compression room. For the expansion valve, orifice equation is utilized [1]. Mass flow rate of the refrigerant is applied to the system as the step input. Afterwars, the dynamic effect of R1234yf and R134a refrigerants to the system's coefficient of performance, required compressor work, cooling load, pressure-enthalpy and temperature-entropy characteristics are investigated.

The rest of the paper is considered as follows. In the second chapter, dynamical modelling of the refrigeration cycle is described. In the third chapter, the results are discussed in detail and the fourth chapter concludes the paper.

MODELLING OF THE SYSTEM

A basic refrigeration cycle consists of four components, namely, the evaporator, the condenser, the compressor and the expansion valve. The refrigerant absorbs the heat from the evaporator and evaporates, then the gas is compressed in the compressor and directly its pressure and indirectly its temperature increases. Afterwards, the excess temperature is emitted in the condenser and the pressure of the refrigerant is decreased to the condenser inlet pressure level in the expansion valve. A diagram of a basic refrigeration cycle is given in Fig. 1.

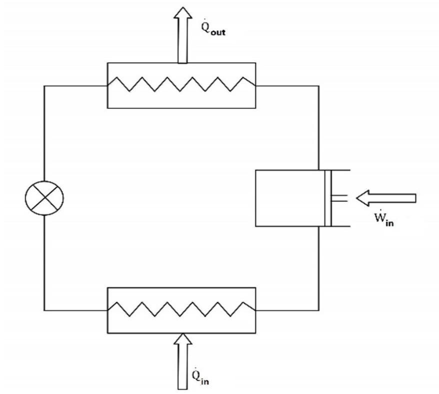

Figure 1. A basic refrigeration cycle

In the following subsections, the dynamical modelling of the each component is given.

Evaporator

The finite difference method is utilized for the modelling of the evaporator. A cross-flow evaporator with one dimensional fluid flow is considered. Gungor and Winterton [16] correlation is utilized for the modelling of the evaporation process. The heat convection coefficient can be calculated with Gungor and Winterton correlation shown in equations through 1-7.

$$Bo = \frac{q}{\rho V h_{fg}} \tag{1}$$

$$X_{tt} = \left(\frac{1-x}{x}\right)^{0.9}\left(\frac{\rho_v}{\rho_l}\right)^{0.5}\left(\frac{\mu_l}{\mu_v}\right)^{0.1} \tag{2}$$

$$E = 1 + 24000 Bo^{1.16} + 1.37(1/X_{tt})^{0.86} \tag{3}$$

$$S = \frac{1}{1 + 1.15x10^{-6} E^2 \mathrm{Re}^{1.17}} \tag{4}$$

$$h_1 = 0.023 \mathrm{Re}^{0.8} \mathrm{Pr}^{0.4} k / d \tag{5}$$

$$h_{pool} = 55 \mathrm{P}_r^{0.12} \left(\log_{10} P_r\right)^{-0.55} M^{-0.5} q^{0.67} \tag{6}$$

$$h_{tp} = E h_1 + S h_{pool} \tag{7}$$

where Bo represents the boiling number, q shows the heat transfer rate, X_{tt} shows the Martinelli coefficient, x represents the quality of the vapor, k shows the heat conduction coefficient, M shows the molar mass and v and l subscripts represents the gas and liquid phases, respectively. Gnielinski [18] correlation is utilized for the single phase turbulent flows. Nusselt number can be calculated with the use of Gnielinski correlation as in Eq. 8.

$$Nu = \frac{(f/2)(\mathrm{Re} - 1000)\mathrm{Pr}}{1 + 12.7\left(\mathrm{Pr}^{2/3}\right)\sqrt{f/2}} \tag{8}$$

where Nu represents the Nusselt number, Pr shows the Prandtl number, Re shows the Reynolds number and f represents the friction factor. The friction factor and the Reynolds number can be calculated by using Eq. 9-11.

$$\mathrm{Re} = \frac{\rho V D}{\mu} \tag{9}$$

$$\begin{aligned} f &= \frac{64}{\mathrm{Re}} && \text{Laminar} \\ f &= \left(0.79 \ln \mathrm{Re} - 1.64\right)^{-2} && \text{Turbulence} \end{aligned} \tag{10}$$

where ρ shows the fluid density, V represents the fluid velocity, D shows the pipe diameter and μ represents the fluid viscosity. The equations for the calculation of the behavior of the primary fluid are given in Eq. 11-12.

$$\frac{\partial \dot{m}_g h_g}{\partial t} = \dot{m}_e h_{fg} - \frac{\partial \dot{m}_g h_g}{\partial x} dx \tag{11}$$

$$\frac{\partial \dot{m}_f h_f}{\partial t} = h_i p_i dx\left(T_{hx} - T_r\right) - \frac{\partial \dot{m}_f h_f}{\partial x} dx - \dot{m}_e h_{fg} \tag{12}$$

where $\dot{m}_f$, $\dot{m}_g$ ve $\dot{m}_e$ shows the mass flow rate of the liquid, gas and liquid-gas phases, respectively, h_f, h_g ve h_{fg} represents the enthalpy of the liquid, gas and liquid-gas phases, respectively, h_i represents the convection coefficient of the fluid, p_i shows the inner tube diamater and T_{hx} and T_r represents the wall and primary fluid temperatures, respectively. The behavior of the secondary fluid can be calculated by utilizing the Eq. 13.

$$\rho\frac{\partial h}{\partial t} - \rho V a \frac{\partial h}{\partial x} - \frac{h_o p_o}{A}\left(T_{hx} - T_f\right) = 0 \tag{13}$$

where ρ shows the fluid density, Va shows the fluid velocity, h_o shows the convection coefficient, p_o represents the outer tube diameter and T_f represents the secondary fluid temperature. The wall temperature of the evaporator can be calculated as Eq. 14

$$C\rho V\frac{\partial T_{hx}}{\partial t} - h_i p_i\left(T_r - T_{hx}\right) + h_o p_o\left(T_{hx} - T_f\right) = 0 \tag{14}$$

where C shows the spesific heat of the wall and V shows the volume of the wall.

Condenser

Modelling of the condenser follows the same procedure of the evaporator except the condensation process is modelled with the Travis et al. [17] correlation. The wall and the secondary fluid behavior equations of the evaporator are valid for the condenser. Primary fluid behavior of the condenser can be calculated as the following equations.

$$\frac{\partial \dot{m}_f h_f}{\partial t} = \dot{m}_c h_{fg} + \frac{\partial \dot{m}_f h_f}{\partial x} dx \tag{15}$$

$$\frac{\partial \dot{m}_g h_g}{\partial t} = h_o p_o dx\left(T_r - T_{hx}\right) + \frac{\partial \dot{m}_g h_g}{\partial x} dx + \dot{m}_c h_{fg} \tag{16}$$

where $\dot{m}_c$ shows the mass flow rate of the condensing fluid.

Compressor

Modelling of the compressor is achieved in two separate processes. First, the heat transfer between the fluid and the environment is considered until the fluid arrives to the compression room. Then, the polytropic compression process equation is utilized after the refrigerant arrives to the compression room. An example demonstration of the compressor is given in Fig. 2.

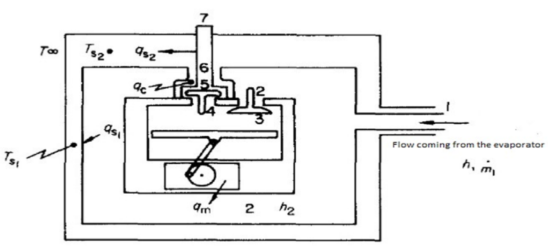

Figure 2. Inner design of the compressor [1]

The heat transfer equations that models the fluid temperature change until the fluid arrives to the compression room are given in Eqs. 17-19.

$$\rho_{fl} V_{fl}\left(T_3 - T_1\right) = h_{co}\left(T_{cyl} - T_1\right) - h_{s1}\left(T_1 - T_{s1}\right) \tag{17}$$

$$\left(C_{cyl}\rho_{cyl}V_{cyl}\right)\frac{dT_{cyl}}{dt} = h_{ci}\left(T_5 - T_{cyl}\right) - h_{co}\left(T_{cyl} - T_1\right) \tag{18}$$

$$\left(C_{sh}\rho_{sh}V_{sh}\right)\frac{dT_{s1}}{dt} = h_{s1}\left(T_2 - T_{s1}\right) - h_{s1o}\left(T_{s1} - T_{\infty}\right) \tag{19}$$

where *fl, cyl* ve *sh* subscripts shows the primary fluid, the cylinder and the outer shell of the compressor. Meanings of the other symbols and subscripts can be inferred from Fig. 2. The fluid enters the compressor in T_1 temperature, then, it interacts with the environment and heats up to T_3 temperature and compressed in the compression room. Compression process in the compression room can be represented by the following equation.

$$\frac{T_4}{T_3} = \left(\frac{P_{cond}}{P_{evap}}\right)^{\frac{\gamma-1}{\gamma}} \tag{20}$$

where T_4 shows the compressor outlet temperature, P_{cond} and P_{evap} represents the condenser and the evaporator pressures and γ shows the isentropic compression coefficient.

Expansion valve

The modeling of the expansion valve is accomplished by utilizing the orifice equation given in James and James [19]. The fluid enthalpy is assumed to be steady between the enterance and exit of the expansion valve. The orifice equation is given in Eq. 21.

$$\dot{m} = 0.0683x\sqrt{\left(P_{cond} - P_{evap}\right)} \tag{21}$$

where x shows the openness measure of the valve needle in mms.

RESULTS

Mass flow rate of the primary fluid with 0.2 kg/sec is applied to the system as step input. The input is applied to the system from the enterance of the evaporator and after each cycle completion, a time step is executed. R134a and R1234yf are utilized as the primary fluids and water is utilized as the secondary fluid. Thermodynamic and thermophysical property equations of R134a, R1234yf and water are acquired from Tillner-Roth and Baehr [20], Richter et al. [21] and Wagner and Pruβ [22], respectively. Isentropic compression ratios of R134a and R1234yf are considered as 1.2 and 1.1, respectively. Walls of the evaporator and the condenser and shell of the compressor are considered as made of steel. Internal pressure of the evaporator is taken as 200 kPa and openness amount of the expansion valve needle is taken as 1.1 mm. By utilizing the orifice equation, it is calculated that the internal pressure of the condenser is 796.6 kPa. Under these circumstances, R134a boils at approximately -10°C and condenses at 31°C, while R1234yf boils at -13°C and condenses at 30.5°C. Inner and outer tube diamaters of the evaporator and the condenser are considered as 0.01m. and 0.018 m. while their lenghts are taken as 14 m. Flow velocity of the both fluids are taken as 0.7 m/sec., under this circumstance, they both flow in turbulence. Initial temperatures of the environment, outer shell of the compressor and the cylinder are taken as 25°C and corresponding convective heat transfer coefficients are selected. In the evaporator, initial temperatures of the primary fluid, the secondary fluid and the wall are considered as -11°C, 0°C and 0°C, while in the condenser, the secondary fluid and the wall initial temperatures are considered as 23°C and 23°C. Finally, time steps are taken as 3 sec. and length steps in the evaporator and the condenser are taken as 0.1 m. Moreover, pressure drops in the evaporator and the condenser, kinetic and potential energy changes are neglected in the simulation and it is assumed that there are no leakings at the pipe connections and no heat loss to the environment from all equipments.

The simulation is accomplished in the Java programming language and contains 600 sec. time frame. The temperature-entropy (T-s) and the pressure-enthalphy (p-h) diagrams at the initial and the final states are given in Fig 3, Fig. 4, Fig. 5, and Fig. 6.

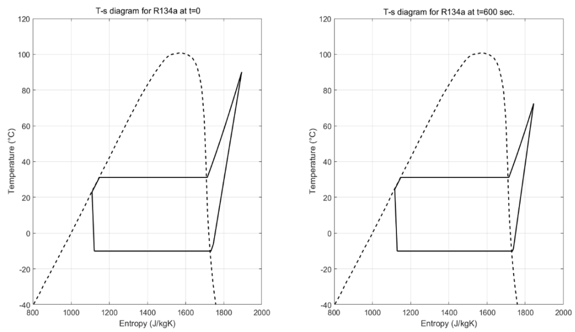

Figure 3. Temperature-entropy diagram for R134a at initial and final states

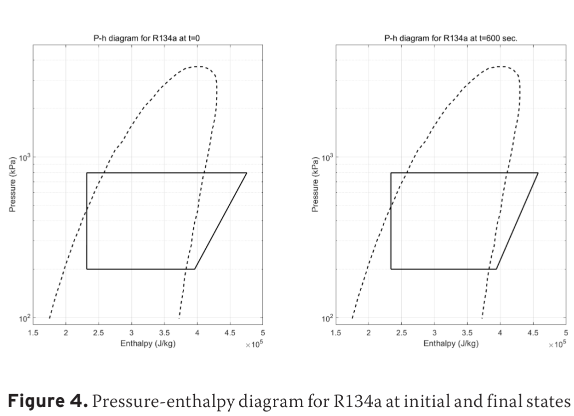

Figure 4. Pressure-enthalpy diagram for R134a at initial and final states

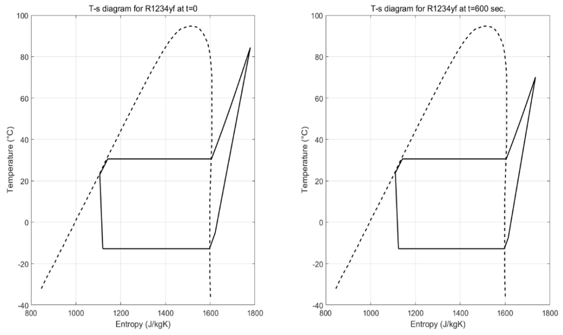

Figure 5. Temperature-entropy diagram for R1234yf at initial and final states

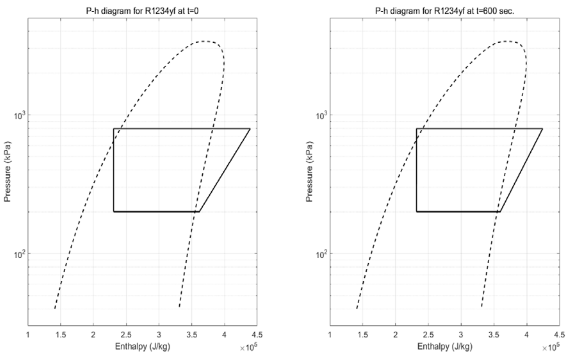

Figure 6. Pressure-enthalpy diagram for R1234yf at initial and final states

By looking at the the Fig. 3, it is seen that, for R134a, the evaporator-, the compressor- and the condenser- outlet temperatures are initially -6.17°C, 90.07°C and 23°C, respectively and finally, they reach to -8.51°C, 71.85°C and 24.47 °C. By looking at the the Fig. 5, it is seen that, for R1234yf, the evaporator-, the compressor- and the condenser- outlet temperatures are initially -5.15°C, 84.37°C and 23.01°C , respectively and finally, they reach to -7.45°C, 70.08°C and 23.86°C. By looking at these results, it can be seen that, the condenser and the evaporator wall temperature changes over time and thus the superheat and the subcool temperatures are decreased and increased, respectively, over time. Also, the compressor outlet temperature is decreased due to the heat transfer from the shell and the environment. The condenser and the evaporator temperatures are tend to get inside of the saturation dome. After these temperatures get inside of the dome, the system loses stability and the COP drops to zero. Variations of the COP, required compressor work and the cooling load over time for both R134a and R1234yf are given in Fig. 7, Fig. 8 and Fig. 9, respectively.

As can be seen in figures, since the superheat temperature decreases over time, required compressor work also decreases. Moreover, the zig-zags in the heat transfer behavior over time of the evaporator occur because of the

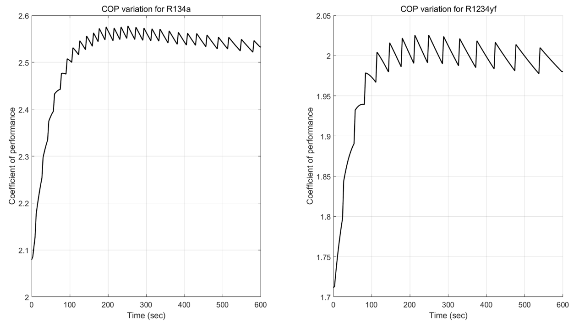

Figure 7. COP variation over time for R134a and R1234yf

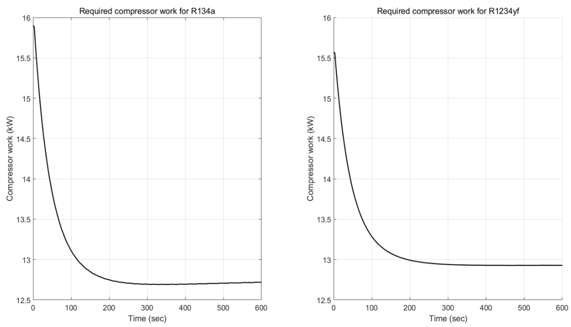

Figure 8. Required compressor work variation over time for R134a and R1234yf

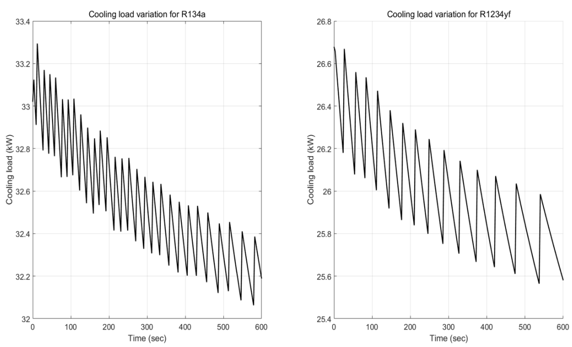

Figure 9. Cooling load variation over time for R134a and R1234yf

instabilities in the evaporation correlation. It can be seen in Fig. 9 that R134a absorbs more heat from the evaporator, however it requires similar amount of compressor work with R1234yf. Therefore, it can be concluded that performance of R134a is greater than R1234yf. The performance comparison is given in Fig. 7. This phenomena occurs because the thermodynamic and thermophysical properties of R134a is more favorable than R1234yf's. The system coefficient of performance ripples because of the zig-zags in the heat absorbtion from the evaporator and after a small overshoot, it slowly decreases. After the superheat temperature drops below zero, the COP value rapidly converges to zero.

M.S. Turgut, M.T. Coban / Hittite J Sci Eng, 2018, 5 (Special Issue: Selected Papers from the 21st National Thermal Sciences and Technology Congress) 09–14

CONCLUSION

In this study, the dynamic behavior of a vapor compression cycle with R134a and R1234yf working fluids is investigated. Modelling of the evaporator and the condenser is achieved with the finite difference method. Modelling of the compressor is accomplished with first, finite difference method, then the isentropic compression equation. Finally, modelling of the expansion valve is done with the orifice equation. The simulation results showed that the evaporator and the compressor wall temperatures decrease and increase, respectively, over time. Therefore, the superheat and the subcool temperatures decrease and increase, respectively, over time. After the the superheat and the subcool temperatures drops below zero, the system loses stability. Also, it is found that, the performance of R134a is better than R1234yf and required compressor work of the system and the heat absorption from the evaporator decreased over time. The coefficient of performance slowly decreased after a small overshoot. The authors plan to study on control algorithms that can maximize the system coefficient of performance in the future works.

References

1. MacArthur JW. Transient heat pump behaviour: a theoretical investigation. Internlational Journal of Refrigeration 7 (1984) 123–132.
2. Yataganbaba A, Kilicarslan A, Kurtbas I. Exergy analysis of R1234yf and R1234ze as R134a replacements in a two evaporator vapour compression refrigeration system. International Journal of Refrigeration 60 (2015) 26–37.
3. Chi J. DEPAC– a computer model for design and performance analysis of central chillers. ASME Paper No 77–HT–11, 1979.
4. Chi J. Computer simulation of fossil–fuel–fıred hydronic boilers, Second ASHRAE HVAC Equipment, 1976.
5. Bonne, U, Patani, A. Modelling the influence of heat pump sizing, climate and test conditions on seasonal efficiency. Conference on HVAC Equipment and Systems, Purdue University, West Lafayette, Indiana, USA, 1978.
6. Dhar, M, Soedel, W, Transient analysis of a vapor compression refrigeration system. XV International Congress of Refrigeration, Venice, Italy, 1979.
7. Ellison RD, Creswich FA. A computer simulation of steady–state performance of air–to–air heat pumps, Oak Ridge National Laboratory Report ORNL/CON–1G, 1978.
8. Chi J, Didion D. A simulation model of the transient performance of a heat pump. International Journal of Refrigeration 5 (1982) 176–184.
9. Bonne, U, Patani, A, Jacobson, R, Muller, D. Electric–driven heat pump system: simulation and controls, ASHRAE Trans. LA–80–5 Los Angeles, California, 1980.
10. Chen ZJ, Lin W. Dynamic simulation and optimal matching of a small–scale refrigeration system. International Journal of Refrigeration 14 (1991) 329–335.
11. Fu L, Ding G, Zhang C. Dynamic simulation of air–to–water dual–mode heat pump with screw compressor. Appl.ied Thermal Engineering 23 (2003) 1629–1645.
12. Madani H, Claesson J, Lundqvist P. Capacity control in ground source heat pump systems part II: Comperative analysis between on/off controlled and variable capacity systems. International Journal of Refrigeration 34 (2011) 1934–1942.
13. Zhu Y, Jin X, Du Z, Fan B, Fu S. Generic simulation model of multi–evaporator variable refrigerant flow air conditioning system for control analysis. International Journal of Refrigeration 36 (2013) 1602–1615.
14. Mota–Babiloni A, Navarro–Esbri J, Barraggan A, Moles F, Peris B. Drop–in energy performance evaluation of R1234yf and R1234ze(E) in a vapor compression system as R134a replacements. Applied Thermal Engineering 71 (2014) 259–265.
15. Belman–Flores JM, Rodriguez–Munoz AP, Perez–Reguera G, Mota–Babiloni A. Experimental study of R1234yf as a drop–in replacement for R134a in a domestic refrigerator. International Journal of Refrigeration 81 (2017) 1–11.
16. Güngör KE, Winterton RHS. A general correlation for flow boiling in tubes and annuli. International Journal of Heat and Mass Transfer 29 (1985) 351–358.
17. Travis DP, Baron AG, Rohsenow WM. Forced–convection condensation inside tubes. MIT Heat Transfer Laboratory, 74, 1971.
18. Gnielinski V. New equations for heat and mass transfer in turbulent pipe and channel flow. International Journal of Chemical Engineering 16 (1976) 359–368.
19. James KA, James RW. Transient analysis of thermostatic expansion valves for refrigeration system evaporators using mathematical models. Transactions of the Institute of Measurement and Control 9 (1987) 350–355.
20. Tillner–Roth R, Baehr HD. A international standard formulation for the thermodynamic properties of 1,1,1,2–Tetrafluoroethane (HFC–134a) for temperatures from 170K to 455K and pressures up to 70 MPa. Journal of Physical & Chemical Reference Data 23 (1994) 657–729.
21. Richter M, McLinden MO, Lemmon EW. Thermodynamic properties of 2,3,3,3–Tetrafluoroprop–1–ene (R1234yf): Vapor pressure and p–ρ–T measurement and equation of state. Journal of Chemical & Engineering Data 56 (2011) 3254–3264.
22. Wagner W, Prup A. The IAPWS formulation 1995 for the thermodynamic properties of ordinary water substance for general and scientific use. Journal of Physical & Chemical Reference Data 31 (2002) 387–535.

M.S. Turgut, M.T. Coban / Hittite J Sci Eng, 2018, 5 (Special Issue: Selected Papers from the 21st National Thermal Sciences and Technology Congress) 09–14